Preparation, Structure, and Bonding in an Organoactinide Imide, $Cp_3AnNPPh_3$ (An = U, Th): A Comparison of the Bonding of Uranium to N- and O-Donor Ligands

Roger E. Cramer,*† Frank Edelmann,† Arthur L. Mori,† Steven Roth,† John W. Gilje,*† Kazuyuki Tatsumi,*‡ and Akira Nakamura‡

Chemistry Department, University of Hawaii, Honolulu, Hawaii 96822, and Department of Macromolecular Science, Faculty of Science, Osaka University, Toyonaka, Osaka 560, Japan

Received June 17, 1987

The reaction of Cp_3AnCl (An = U or Th) with $LiNPPh_3$ produces $Cp_3AnNPPh_3$. The structure of Cp_3UNPPh_3 has been determined by X-ray crystallography (space group $P2_1/c$, a = 10.974 (7) Å, b = 17.022 (3) Å, c = 16.049 (3) Å, β = 114.77 (4)°, Z = 4, V = 2722 (2) Å^3, R = 0.068, and R_g = 0.1063). The U–N bond is very short, 2.07 (2) Å; a near triple bond is suggested by comparisons with transition-metal–imide and –phosphine imide complexes. U–N multiple bonding finds support from extended Hückel molecular orbital calculations on Cp_3UNPH_3, Cp_3UNPh, $Cp_3UNCHCHPH_3$, Cp_3UNH_2, and $Cp_3UNH_3^+$ and on an analogous series of Cp_3U complexes of O-donor ligands. Both U–N or U–O overlap populations correlate linearly with observed U–N or U–O distances, respectively. These results indicate the usefulness of covalent arguments in understanding the structure and bonding of actinide complexes. The very short U–N bond in Cp_3UNPPh_3 is contrasted with the long U–O bond in the analogous phosphine oxide complex, and the difference is rationalized in terms of the bonding abilities of the two ligands.

Imido ligands, $:\ddot{N}R^{2-}$, can donate as many as three electron pairs upon coordination to a metal and are good ligands toward electron-poor, high-valent transition metals.[1] Consequently, imides may be particularly valuable ligands with the early actinides whose chemistry is dominated by the higher oxidation states. At present actinide imides are almost unknown; we reported[2] the first of these, $Cp_3UNC(Me)CHPMePh_2$ (Cp = η^5-C_5H_5, Me = CH_3, Ph = C_6H_5), in 1984, and only Cp_3UNR (R = Ph and $SiMe_3$) has subsequently appeared.[3] The routes to these complexes, however, are specialized, and no general synthetic schemes have been developed for actinide imides.

Because of our work with actinide–phosphoylide complexes,[4] our attention was drawn to phosphine imides, $[:\ddot{N}PR_3]^-$. Since $[:\ddot{N}PR_3]^-$ is isoelectronic both with phosphine oxides, OPR_3, whose ability to complex high-valent actinides is well-known,[5] and with $[:\ddot{C}HPR_3]^-$, which forms multiple bonds to uranium,[6] phosphine imides also may be valuable ligands in actinide chemistry. Transition-metal phosphine imides are not common. Complexes of Ti, V, Nb, Ta, Mo, W, Re, Fe, Ru, and Os have been reported,[7-20] but their syntheses, which involve Staudinger reactions of metal azides with phosphines,[11,14-16] the addition of phosphines to nitrido complexes,[7-10,16,19,20] ligand exchange between metal halides and (trimethylsilyl)iminophosphines,[12,13] or reduction of a metal nitrosyl with phosphine,[18] do not provide a basis for the syntheses of actinide derivatives. Consequently, we have sought a more general route to metal phosphine imides and have turned to $LiNPPh_3$. While transmetalations using lithio derivatives are common, apparently $LiNPR_3$ has only been used to form a few main-group metal imides.[21] In this paper we report its successful use in the preparation of the actinide imides Cp_3UNPPh_3 and $Cp_3ThNPPh_3$.

Since the structure of Cp_3UNPPh_3 suggested U–N multiple bonding, we analyzed the electronic structure of the model compound Cp_3UNPH_3 by using relativistically parameterized extended Hückel calculations. To place the bond in this compound into the overall framework of U–N bonding, we have also performed calculations on Cp_3UNPh, $Cp_3UNCHCHPH_3$, Cp_3UNH_2, and $Cp_3UNH_3^+$. Since NPH_3^- and OPH_3 are isoelectronic, we extended our theoretical analysis to Cp_3UOPH_3 and to the series Cp_3UOCH_3, $Cp_3UOCHCHPH_3^+$, and Cp_3UOH_2.

Experimental Section

All manipulations were carried out under a dinitrogen atmosphere by using standard vacuum line, Schlenk, and/or drybox

† University of Hawaii.
‡ Osaka University.

(1) (a) Nugent, W. A.; Haymore, B. I. *Coord. Chem. Rev.* **1980**, *31*, 123-175. (b) Dehnicke, K.; Straehle, J. *Angew. Chem., Int. Ed. Engl.* **1981**, *20*, 413-426.
(2) Cramer, R. E.; Panchanatheswaran, K.; Gilje, J. W. *J. Am. Chem. Soc.* **1984**, *106*, 1853-1854.
(3) Brennan, J. G.; Anderson, R. A. *J. Am. Chem. Soc.* **1985**, *107*, 514-516.
(4) Gilje, J. W.; Cramer, R. E.; Bruck, M. A.; Higa, K. T.; Panchanatheswaran, P. *Inorg. Chim. Acta* **1985**, *110*, 139-143.
(5) Keller, C. *The Chemistry of the Transuranium Elements*; Verlag Chemie: Weinheim, 1971; pp 229-235.
(6) (a) Cramer, R. E.; Maynard, R. B.; Paw, J. C.; Gilje, J. W. *J. Am. Chem. Soc.* **1981**, *103*, 3589-3590. (b) Cramer, R. E.; Maynard, R. B.; Paw, J. C.; Gilje, J. W. *Organometallics* **1983**, *2*, 1336-1340.
(7) Griffith, W. P.; Pawson, D. *J. Chem. Soc., Chem. Commun.* **1973**, *418*-419.
(8) Pawson, D.; Griffith, W. P. *Inorg. Nucl. Chem. Lett.* **1974**, *10*, 253-255.
(9) Chatt, J.; Dilworth, J. R. *J. Chem. Soc., Chem. Commun.* **1974**, 517-518.
(10) Pawson, D.; Griffith, W. P. *J. Chem. Soc., Dalton Trans.* **1975**, *417*-426.
(11) Bezler, H.; Straehle, J. *Z. Naturforsch., B: Anorg. Chem., Org. Chem.* **1979**, *34B*, 1199-1202.
(12) Choukroun, R.; Gervais, D.; Dilworth, J. R. *Transition Met. Chem. Weinheim, Ger.* **1979**, *4*, 249-251.
(13) (a) Roesky, H. W.; Seseke, U.; Noltemeyer, M.; Jones, P. G.; Sheldrick, G. M. *J. Chem. Soc., Dalton Trans.* **1986**, 1309-1310. (b) Roesky, H. W.; Katti, K. V.; Seseke, U.; Scholz, U.; Herbst, R.; Egert, E.; Sheldrick, G. M. *Z. Naturforsch., B.: Anorg. Chem., Org. Chem.* **1986**, *41B*, 1509-1512.
(14) Duebgen, R.; Mueller, U.; Weller, F.; Dehnicke, K. *Z. Anorg. Allg. Chem.* **1980**, *471*, 89-101.
(15) Mueller, U.; Duebgen, R.; Dehnicke, K. *Z. Anorg. Allg. Chem.* **1981**, *473*, 115-124.
(16) Dilsworth, J. R.; Neaves, B. D.; Hutchinson, J. P.; Zubieta, J. A. *Inorg. Chem. Acta* **1982**, *65*, L223-L224.
(17) Bezler, H.; Straehle, J. *Z. Naturforsch., B: Anorg. Chem., Org. Chem.* **1983**, *38B*, 317-332.
(18) Mronga, N.; Weller, F.; Dehnicke, K. *Z. Anorg. Allg. Chem.* **1983**, *502*, 35-44.
(19) Dehnicke, K.; Prinz, H.; Kafitz, W.; Kujanek, R. *Liebigs Ann. Chem.* **1981**, 20-27.
(20) Schmidt, I.; Kynast, U.; Hanich, J.; Dehnicke, K. *Z. Naturforsch., B: Anorg. Chem., Org. Chem.* **1984**, *39B*, 1248-1251.

0276-7333/88/2307-0841$01.50/0

techniques. Reagents were of the highest commercially available purity. Solvents were deoxygenated and dried by reflux over sodium benzophenone and were distilled under dinitrogen before use. NMR and mass spectra were recorded on a Nicolet NM-300 and Varian MAT-311 spectrometers, respectively. A Syntex P$\bar{1}$ diffractometer operating at ambient temperature was used to collect the diffraction data. Elemental analyses were obtained from Dornis u. Kolbe Mikroanalytisches Laboratorium, Muelheim, West Germany, and Schwartzkopf Microanalytical Laboratories, Woodside, NY.

Preparation of $LiNPPh_3$. With use of reported procedures[22] $(Ph_3PNH_2)(N_3)$ was prepared by the reaction of PPh_3 with anhydrous HN_3 in diethyl ether. The reaction of $(Ph_3PNH_2)(N_3)$ with PPh_3 at 180–200 °C produces $HNPPh_3$.[22] Following the reaction of $HNPPh_3$ with an equivalent amount of LiMe or LiBu in diethyl ether solution,[21] $LiNPPh_3$ was precipitated by the addition of heptane.

Preparation of Cp_3UNPPh_3. Cp_3UCl (330 mg, 0.70 mmol) and $LiNPPh_3$ (200 mg, 0.71 mmol) were slurried in 20 mL of toluene under a dinitrogen atmosphere. Within a few hours a green-brown solution had formed that became olive green after the mixture had been stirred for about 18 h. Following filtration and evaporation of the filtrate, an olive green residue remained that was redissolved in 10 mL of toluene. After 30 mL of hexane was added to this solution, it was cooled to −20 °C for about 12 h during which Cp_3UNPPh_3 crystallized. The nearly colorless supernatant was separated by filtration, the precipitate was washed with about 10 mL of pentane, and 295 mg (59% yield) of green, crystalline Cp_3UNPPh_3 was obtained. NMR spectrum (300 MHz, toluene-d_8, 23 °C): 18.02 (6 H, d, J_{HCCH} = 7 Hz, Ph ortho) 8.94 (6 H, t, J_{HCCH} = 7 Hz, Ph meta), 8.40 (3 H, t, J_{HCCH} = 7 Hz, Ph para), −21.0 ppm (15 H, s, Cp). EI mass spectrum (25 and 75 eV): peaks for $[(C_5H_5)_3UNP(C_6H_5)_3]^+$, $[(C_5H_5)_2UNP(C_6H_5)_3]^+$, $[(C_5H_5)UNP(C_6H_5)_3]^+$, and $[NP(C_6H_5)_3]^+$. The results of elemental analyses on this compound were scattered. Several samples were submitted and two independent laboratories were utilized. One satisfactory result was obtained: Anal. Calcd for $C_{33}H_{30}PNU$: C, 55.85; H, 4.26; N, 1.97. Found: C, 55.84; H, 4.22; N, 1.96. Other analyses gave reasonable nitrogen and hydrogen but low, irreproducible carbon values.

Preparation of $Cp_3ThNPPh_3$. Cp_3ThCl (1.04 g, 2.25 mmol) and $LiNPPh_3$ (0.700 g, 2.45 mmol) were slurried in 30 mL of toluene under a dinitrogen atmosphere. The mixture was stirred for 24 h. During this period a black precipitate formed, apparently reflecting partial reduction of Cp_3ThCl to finely divided thorium metal. A clear yellow solution was obtained following filtration with the aid of Celite through a medium-porosity glass frit. Evaporation of volatile components left a tan residue which was washed with hexane and dried in vacuo, and 0.926 g (57% yield) of $Cp_3ThNPPh_3$ was obtained. This material can be further purified by recrystallization as described for Cp_3UNPPh_3. NMR spectrum (300 MHz, THF-d_8, 23 °C): 7.7 (6 H, mult, Ph ortho), 7.5 (9 H, mult, Ph meta, para), 6.21 ppm (15 H, s, Cp). EI mass spectrum (10 eV): peaks for $[(C_5H_5)_3ThNP(C_6H_5)_3]^+$, $[(C_5H_5)_3Th]^+$, $[ThNP(C_6H_5)]^+$, and $[NP(C_6H_5)_3]^+$. Satisfactory elemental analysis was not obtained for this compound. Several samples were submitted for analysis, and scattered irreproducible results were obtained even on identical samples submitted at the same time. Nitrogen values were obtained that were in the correct range, but hydrogen was typically somewhat high and carbon low.

Collection and Reduction of X-ray Data. A crystal of Cp_3UNPPh_3 from the preparation described above was selected and mounted in a thin-walled glass capillary under dinitrogen. Crystal, data collection, and refinement parameters are listed in Table I, and the instrumentation, procedures, and programs used have been previously described.[6b] Cell constants were determined by least-squares methods from the centered angular coordinates of 15 intense reflections with 2θ values between 31.8° and 41.7°. Atomic scattering factors for P^0, N^0, C^0, and H^0 were supplied by SHELX-76.[23a] The atomic scattering factor including the anomolous dispersion correction for U^0 was taken from the literature.[24] The data was corrected for absorption by using the program PROCESS[23b] and measured ψ scans for four reflections with χ values $80° < \chi < 90°$.

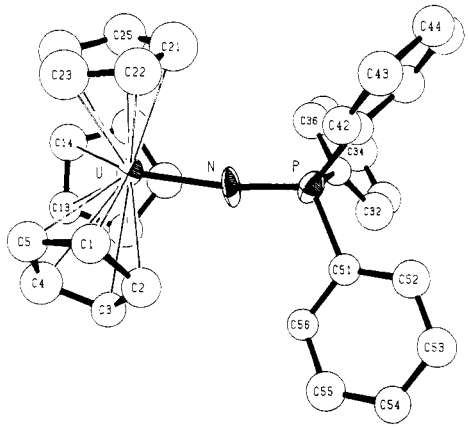

Figure 1. An ORTEP drawing of Cp_3UNPPh_3.

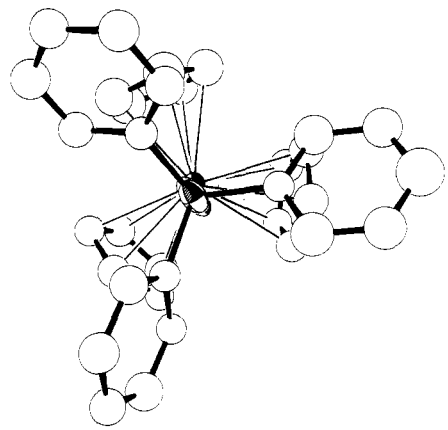

Figure 2. An ORTEP drawing of Cp_3UNPPh_3 down the U–N–P axis.

Structure Solution and Refinement. The structure was solved in space group $P2_1/c$, which was indicated by systematic absences. The position of the uranium atom was determined by Patterson methods, and the remaining atoms were located in a straightforward fashion in a series of difference Fourier maps and least-squares refinements by using SHELX-76. The uranium, nitrogen, and phosphorus atoms were refined anisotropically and the cyclopentadienide and phenyl groups as rigid groups with fixed 0.95-Å C–H bonds by using the parameters contained in SHELX-76. Refinement converged at $R_1 = 0.068$ and $R_2 = 0.106$. In the last cycle of refinement no parameter shifted more than 8% of its estimated standard deviation. A final difference Fourier map showed maximum peaks of 2.29–3.72 e/Å^3 near the uranium atom.

The positional and thermal parameters of the non-hydrogen atoms are in Table II and those for the hydrogen atoms in Table III (supplementary material). Observed and calculated structure factors are in Table IV (supplementary material).

Results and Discussion

The reaction of Cp_3AnCl with $LiNPPh_3$ produces $Cp_3AnNPPh_3$ (eq 1). These materials are soluble in THF

$$Cp_3AnCl + LiNPPh_3 \rightarrow Cp_3AnNPPh_3 + LiCl \quad (1)$$

and aromatic hydrocarbons. They are stable for long periods of time when stored under anaerobic anhydrous

(21) Schmidbaur, H.; Jonas, G. *Angew. Chem., Int. Ed. Engl.* **1967**, *6*, 449–450; *Chem. Ber.* **1967**, *100*, 1120–1128; *Chem. Ber.* **1968**, *101*, 1271–1285.

(22) Appel, R.; Koehnlein, G.; Schoellhorn, R. *Chem. Ber.* **1965**, *98*, 1355–1368.

(23) (a) SHELX-76, a system of computer programs for X-ray structure determination by G. M. Sheldrick, 1976. (b) PROCESS, a computer program for Lorenz, polarization, and empirical absorption correction of diffraction data, obtained from Prof. R. Bau, University of Southern California, and modified by M. Carrie, University of Hawaii, 1986.

(24) *International Tables for X-Ray Crystallography*; Kynoch: Birmingham, England, 1967; Vol. 4, pp 101, 150.

Table I. Crystal, Data Collection, and Reduction Parameters for Cp_3UNPPh_3

formula: $(C_5H_5)_3UNP(C_6H_5)_3$	fwt: 709.613
space group (and No.): $P2_1/c$ (No. 14)	cryst system: monoclinic
lattice constants with esd's	
a, Å: 10.974 (7)	α, deg: 90
b, Å: 17.022 (3)	β, deg: 114.77 (4)
c, Å: 16.049 (3)	γ, deg: 90
no. of molecules per unit cell, Z: 4	V, Å^3: 2722 (2)
cryst dimen, mm: 0.76 × 0.36 × 0.32	cryst shape: monoclinic
cryst vol, mm^3: 0.088	cryst color: green
D(calcd): 1.732 g/cm^3	
abs coeff, μ, cm^{-1}: 57.6	
abs corr range: 1.00–1.93	
radiatn: Mo Kα	wavelength, Å: 0.71073
scan type: 2θ	scan rate, deg/min: 2–24
2θ range: 3–50	
total observns: 4313	no. of data used in refinement: 2957
criteria for selecting data used in refinement: $I > 3\sigma(I_o)$	
no. of Parameters: 98	overdetermination ratio: 30.2
final R: 0.068	R_g: 0.1063

$R = \sum(|F_o - F_c|)/\sum(F_o)$

$R_g = [\sum(|F_o - F_c|^2)/\sum(F_o^2)]^{1/2}$

conditions but decompose rapidly when exposed to moisture or oxygen.

Because the actinide imides are not a well-studied class of compounds, the crystal structure of Cp_3UNPPh_3 was determined. ORTEP drawings are shown in Figures 1 and 2, and bond distances and angles are summarized in Tables V and VI, respectively. The geometry about both the uranium and phosphorus is the usual distorted tetrahedron. The average U–C(Cp) distance, 2.78 (2) Å, is in the range reported for other Cp_3U–X complexes,[6] and the $NPPh_3^-$ ligand does not significantly differ from those in transition-metal–phosphine imide complexes which contain a nearly linear M–N–P linkage.[11,16,25] The P–N bond distance, 1.61 (2) Å, is not significantly different from 1.630 (8) Å in $(Ph_3PN)ReCl_3(NO)(OPPh_3)$[18] and 1.609 (8)° in $F_4W(NPMe_3)_2$,[13b] where the Re–N–P angles are 138.5 (5)°[18] and 139.1 (4)°,[13b] respectively, and 1.615 (6) Å[26] in $[H_2NPPh_3]^+$. The most interesting features of the structure are the U–N bond distance of 2.07 (2) Å and the eclipsed conformation of the Cp_3U and PPh_3 groups about the U–N–P axis.

Some U–N and U–C bond distances are compared in Table VII. Here the uranium oxidation state, the ligand charge, and the number of ligand lone pairs have been assigned from the point of view of an ionic model, i.e. by considering a heterolytic cleavage of the metal–ligand bond. In terms of a strictly ionic model the distance to uranium of equally charged ligands should be about the same, with the U–N separations being, perhaps, a few percent shorter than the U–C distances. However, data from Table VII show poor correlation between oxidation state, ligand charges, and bond length. Rather there is an obvious correlation between bond length and the number of ligand electron pairs that are available for metal–ligand bonding.

If electron delocalization does not occur within the R group, the bonding in transition-metal imide complexes can be described in terms of the resonance forms:[1]

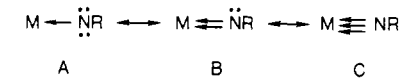

A B C

When the electron count about the metal allows donation of three electron pairs from nitrogen, the contribution from A and B is usually minor and the metal–nitrogen bond order is nearly 3. In such complexes the metal–nitrogen triple bond is 0.41 ± 0.02 Å longer than the appropriate Pauling metallic radius.[1a] While the metallic radius of four valent uranium has not been tabulated by Pauling,[27] 1.60 Å can be estimated by subtracting the difference in ionic radii[28] between U(IV) and Th(IV), 0.05 Å, from the metallic radius of thorium, 1.65 Å. Subtraction of 1.60 Å from the U–N bond distance, 2.02 Å, in Cp_3UNPh[3] yields 0.42 Å, which agrees with the value for the transition-metal imides.

The metal–nitrogen bond distances in structurally characterized phosphine imide complexes are summarized in Table VIII. Four of these compounds show differences between the M–N distances and the Pauling metallic radii that are greater than 0.50 Å. Two of these, $(Ph_3PO)(ON)Cl_3ReNPPh_3$ and $(Et_2PhP)_2Cl_3RuNPPhEt_2$, would have a metal electron count of 20 if the NPR_3^- ligand serves as a three-electron pair donor. According to the criteria suggested by Nugent and Haymore,[1a] the metal–nitrogen bonds in these compounds should be at most double bonds, and the approximate 0.60-Å difference between M–N distance and metallic radius is reasonable for an metal–nitrogen bond order of about 2.[1a] Likewise, since a 20-electron complex would result if both NPR_3^- ligands in $F_4W(NPPh_3)_2$ or $F_4W(NPMe_3)_2$ donate three electron pairs, a W–N bond order of at most 2.5 would be expected for these complexes. The 0.52-Å difference between the W–N distance and the Pauling metallic radius of W is consistent with a bond order of about 2.25[1a] and may indicate that the W–F bonds within these complexes also have some multiple-bond character.

There are no obvious reasons why the other complexes in Table VIII should not form metal–nitrogen triple bonds. In fact, the differences between M–N distances and metallic radii for them are all nearly the same, somewhat larger than 0.41 Å expected[1a] for a triple bond, but less than 0.48 Å for a bond order of 2.5.[1a] These values argue for the importance of H (see below) in the bonding of this group of compounds. Since the differences of bond length and metallic radii for Cp_3UNPh and Cp_3UNPPh_3 coincide with values calculated for related transition-metal complexes, a resemblance is implied between the uranium–nitrogen bonds in the imide and phosphine imide complexes and analogous transition-metal–nitrogen bonds.

The description of the bonding in phosphine imide complexes requires the consideration of several resonance structures:

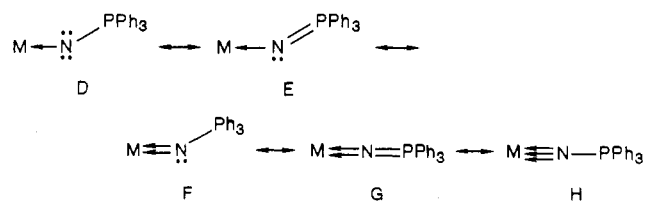

D E F G H

Two resonance forms

(25) Philips, F. L.; Skapski, A. C. *J. Chem. Soc., Dalton Trans.* **1976**, 1448–1450.

(26) Hursthouse, M. B.; Walker, N. P. G.; Warrens, C. P.; Woollins, J. D. *J. Chem. Soc., Dalton Trans.* **1985**, 1043–1047.

(27) Pauling, L. *The Nature of the Chemical Bond*, 3rd. ed., Cornell University Press: Ithaca, NY, 1960.

(28) Shannon, R. D. *Acta Crystallogr., Sect. A.: Cryst. Phys., Diffr., Theor. Gen. Crystallogr.* **1976**, *A32*, 751–767.

$$[:\ddot{N}-PR_3]^- \longleftrightarrow [:N\equiv PR_3]^-$$
I J

should be most important in describing the electronic structure of the NPR_3^- ligand. Extended Hückel molecular orbital calculations yield the charges shown in Figure 6 and show that a high negative charge resides on N while the neighboring P atom assumes a large positive charge. This highly polarized N–P bond indicates that the phosphonium-type resonance form, I, is more appropriate than the phosphorane-type, J, in describing the local bond nature within the NPR_3^- ligand. In addition, high-quality calculations[29] indicate that the isoelectronic $CHPR_3^-$ is best described as a phosphonium dicarbanion, $[:\ddot{C}H-PR_3]^-$, and semiempirical calculations and experimental data on $HNPR_3$ have been interpreted[30] in terms of $H\ddot{N}-PR_3$ being more important than $H\ddot{N}=PR_3$. The importance of I indicates that NPR_3^- is potentially a three-electron pair donor and implies that H can be important in the bonding of phosphine imide complexes.

Further support for the idea of multiple bonding in Cp_3UNPPh_3 comes from NMR data. The chemical shifts of the Cp groups in paramagnetic Cp_3UX molecules occur between about −4 to −21 ppm. Fischer[31] has proposed that these chemical shifts can be related to the U–X bond character and that multiple bonding induces upfield chemical shifts. In terms of this correlation the Cp resonance of Cp_3UNPPh_3, −21.0 ppm, is at the extreme upfield end of this range as would be expected for a triple U–N bond.

Molecular Orbital Analysis. To gain further insight into the nature of the short U–N bond in Cp_3UNPPh_3, we have calculated the electronic structure of the model compound Cp_3UNPH_3. In addition we have probed the factors that contribute to U–N bond distances by analyzing the bonding in Cp_3UNPh, $Cp_3UNCHCHPH_3$, Cp_3UNH_2, and $Cp_3UNH_3^+$. Our molecular orbital calculations are based on the quasi-relativistic extended Hückel method. Computational details are described in the Appendix.

The Nature of the U–N Bond. Figure 3 shows the potential energy curve (top) and the U–N overlap populations (bottom) calculated for Cp_3UNPH_3 as a function of the U–N–P angle, θ. It is evident that the linear geometry is favored energetically. In this conformation U–N overlap population is maximized; it decreases as U–N–P bends. A simple explanation for this behavior is that p_π–p_π, d_π–p_π, and/or f_π–p_π overlaps are optimized at θ = 180°. However, the computed potential well is not very steep, particularly near θ = 180°. Consequently, a slight bending of the U–N–P spine to relieve, for example, steric interactions only results in a slight loss in U–N bond strength.

In Figure 4 the molecular orbitals for Cp_3UNPH_3 are constructed by allowing Cp_3U^+ and NPH_3^- fragments to interact. The frontier orbitals of Cp_3U^+ have already been discussed.[3,32] The fragment orbitals that are concentrated on the Cp^- ligands do not interact with the NPH_3^- orbitals, and, for clarity, these have been omitted from Figure 4 where the remaining Cp_3U^+ frontier orbitals are shown on

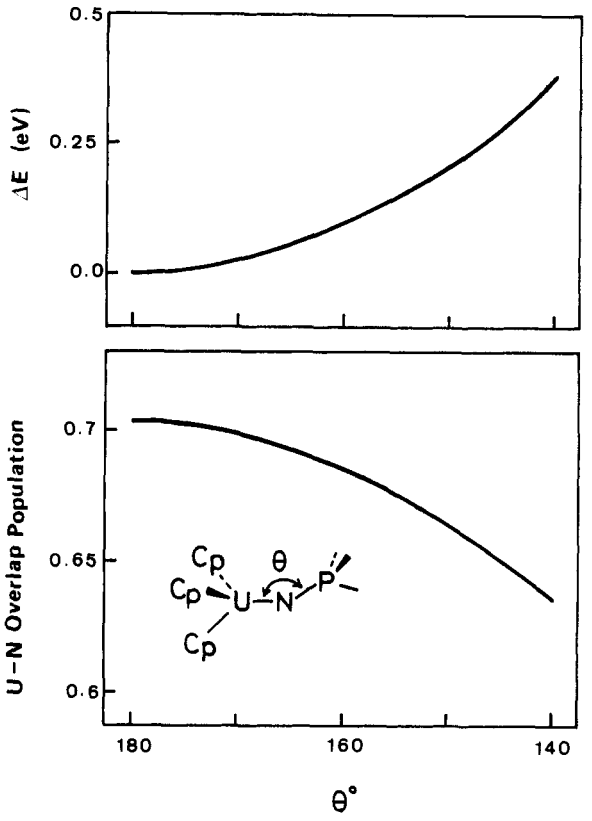

Figure 3. Potential energy curve and change in the U–N overlap population calculated for Cp_3UNPH_3 as a function of the U–N–P angle θ.

the left. The upper five orbitals have mainly U 6d character. At highest energy are the degenerate $x^2 - y^2$ and xy orbitals, 9e. The 8e set is composed largely of xz and yz but has some 7p character that results in the main lobes of 8e pointing away from the three Cp^- ligands. Next is $6a_1$ which consists of z^2 hybridized with 7s and 7p. At lower energy there is a group of seven U 5f orbitals. Reflecting uranium's formal IV oxidation state, two electrons reside in the f block. With exception of $2a_2$, which is nearly pure $y(3x^2 - y^2)$, the low C_{3v} symmetry of Cp_3U^+ does not allow us to assign these orbitals using the familiar representation based on the general f set.[33] Rather, the f_σ orbital, z^3, splits into $3a_1$ and $4a_1$, while the f_π orbitals xz^2 and yz^2 appear in both 4e and 5e.

The two π and one σ lone-pair frontier orbitals of NPH_3^- are depicted on the right side of Figure 4. They are fully occupied by electrons in the monoanion. Since the π orbitals are made of 91% nitrogen p_x and p_y, charge separation occurs within the ion with a large negative charge of −2.2 e on N and a +1.0 e positive charge on P. As shown in Figure 4, the Cp_3U^+ group orbitals that interact with the NPH_3^- π orbitals are 8e, 5e, and 4e. The latter two orbitals are within the f block, and their interactions arise from N x–U xz^2 and N y–U yz^2 overlaps. The U–N σ bond forms through interactions between the NPH_3^- n orbital and the $6a_1$, $4a_1$, and $3a_1$ orbitals of Cp_3U^+. In other words, the $z^2 + z$ hybrid ($6a_1$) and the z^3 orbital of U are involved in σ bonding. The resultant U–N σ bonding molecular orbital splits into two because of mixing with the Cp_3–U bonding orbital. The U–N π and σ interactions are schematically drawn in 1 and 2, respectively.

In addition to providing a measure of covalent bond strength, overlap population analysis can provide an in-

(29) (a) McDowell, R. S.; Streitwieser, A., Jr. *J. Am. Chem. Soc.* **1984**, *106*, 4047–4048. (b) Payne, P., Stanford Research Institute, private communication.
(30) Starzewski, K. A. O.; tom Dieck, H. *Inorg. Chem.* **1979**, *18*, 3307–3316.
(31) Fischer, R. D. In *Fundamental and Technological Aspects of Organo-f-Element Chemistry*; Marks, T. J., Fragala, I. L., Eds.; D. Reidel: Boston, 1985; pp 277–326.
(32) Tatsumi, K.; Nakamura, A. *J. Organomet. Chem.* **1984**, *272*, 141–154.
(33) (a) Friedman, H. G., Jr.; Choppin, G. R.; Feuerbacher, D. G. *J. Chem. Educ.* **1964**, *41*, 354–358. (b) Becker, C. *Ibid.* **1964**, *41*, 358–360.

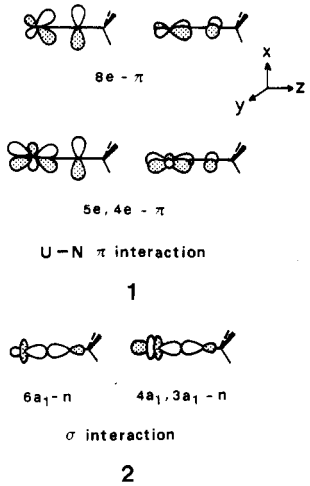

sight into the contributions of individual atomic orbitals to a bond. For Cp_3UNPH_3 the large π component, 0.304 (see Table IX), of the total U–N overlap population, 0.703, supports the idea of multiple U–N bonding in Cp_3UNPH_3. Contribution from the U $7p_\pi$–N p_π and the U $6d_\pi$–N p_π combinations arise primarily from the 8e–π interaction shown in 1, and the U $5f_\pi$–N p_π overlap population is a reflection of the (5e,4e)–π interaction. Among them, the $6d_\pi$ orbitals contribute most to the π bonding with $5f_\pi$ being next most important. The good $6a_1$–n interaction in 2 leads to the large σ-overlap populations associated with U $7p_\sigma$ and $6d_\sigma$ orbitals, while the $5f_\sigma$ contribution is relatively small.[34] The inner-shell 6p orbitals, at −30 eV in energy and not shown in Figure 5, interact with the π and n orbitals of NPH_3^- in an antibonding manner.[34] This results in a negative 6p–n overlap populations and a slight reduction in U–N bond strength.

Our theoretical analysis of Cp_3UNPH_3 has so far been based on the Cp_3U^+ and NPH_3^- groups assuming an eclipsed configuration, 3, similar to that we observe for Cp_3UNPPh_3. To probe electronic reasons for the molecule assuming this conformation, calculations were also performed by using a staggered orientation of these two groups, 4. The results obtained for 4 are almost the same

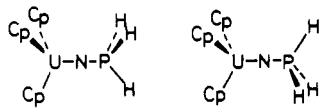

as those for 3. The molecular orbital levels and overlap populations are nearly identical between 3 and 4. Only the very small energy difference of 0.002 eV favors 3. Thus our interpretation of the bonding in 3 carries over to the staggered geometry, and we are unable to provide a compelling reason for the conformational preference of Cp_3UNPPh_3.

Having analyzed the bonding in Cp_3UNPH_3, we compare it with other known U–N bonds. A number of uranium complexes with N-donor ligands have been structurally characterized. Their U–N bond distances are surprisingly diverse[35] and range from 2.019 (6) Å in Cp_3UNPh^3 to 2.678 (16) Å in $Cp_3U(NCS)(NCMe)$.[36] Cp_3UNPPh_3 has one of the shortest distances, in qualitative agreement with its assignment as a nearly triple bond. We chose to perform further calculations on

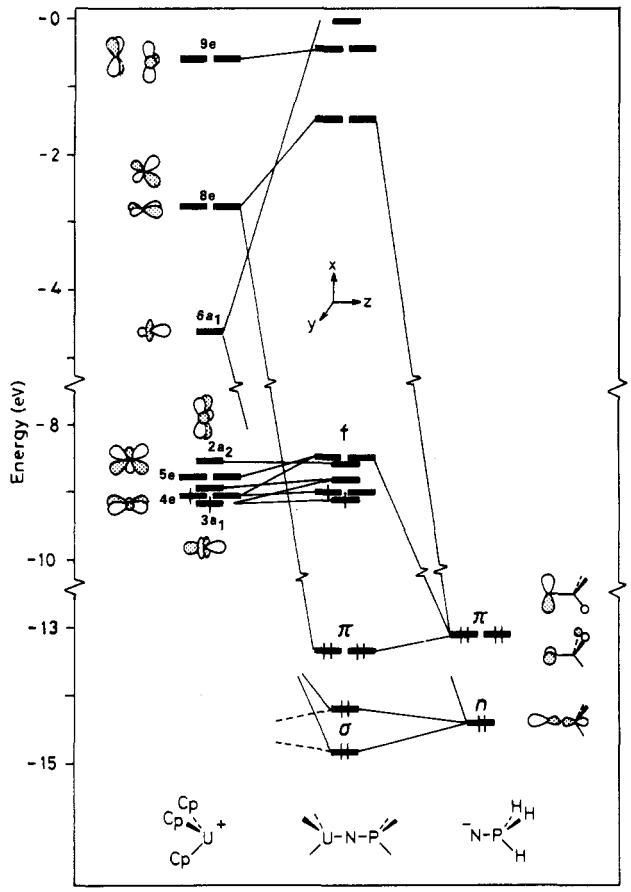

Figure 4. Interaction diagram for the valence orbitals of Cp_3U^+ and NPH_3^- in the eclipsed conformation. Numbering given for the Cp_3U^+ obitals was taken from the previous work,[32] in which $5a_1$, 6e, $3a_2$, and 7e molecular orbitals, which lie between −6 and −8 eV and arise primarily from Cp π and π^* orbitals, were also included.

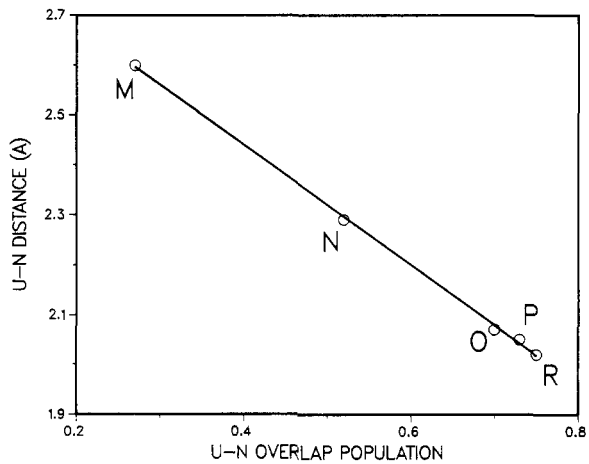

Figure 5. Correlation between the observed U–N distances and the U–N overlap populations calculated at U–N = 2.06 Å: M, $Cp^*_2UCl_2(\eta^1\text{-}N_2C_3H_4)$–$Cp_3UNH_3$; N; Cp_3UNPh_2–Cp_3UNH_2; O, Cp_3UNPPh_3–Cp_3UNPH_3; P; $Cp_3UNC(Me)CHPMePh_2$–$Cp_3UNCHCHPH_3$; R, Cp_3UNPh–Cp_3UNPh.

(34) Other calculations have also shown 6d orbitals to be more important than 5f orbitals in the bonding of organoactinide complexes. See, for example: (a) Bursten, B. E.; Novo-Gradac, K. J. *J. Am. Chem. Soc.* **1987**, *109*, 904. (b) Bursten, B. E.; Strittmatter, R. J. *J. Am. Chem. Soc.* **1987**, *109*, 6606–6608. The 6p orbitals are important in describing the electronic structures of O=U=O^{2+}. (a) Denning, R. G.; Snellgrove, T. R.; Woodwark, D. R. *Mol. Phys.* **1979**, *37*, 1109–1143. (b) Tatsumi, K.; Hoffmann, R. *Inorg. Chem.* **1980**, *19*, 2656–2658 and references therein.

(35) A listing of U–N distances is given in: Cramer, R. E.; Engelhardt, U.; Higa, K. T.; Gilje, J. W. *Organometallics* **1987**, *6*, 41–45.

(36) Fischer, R. D.; Klaehne, E.; Kopf, J. *Z. Naturforsch., B: Anorg. Chem., Org. Chem.* **1978**, *33B*, 1393–1397.

Table II. Positional and Thermal Parameters of Non-Hydrogen Atoms for Cp_3UNPPh_3

Anisotropically Refined Atoms

atom	*x*	*y*	*z*	*U*(11)	*U*(22)	*U*(33)	*U*(12)	*U*(13)	*U*(23)
U	−0.8373 (1)	−0.2121 (1)	−0.9374 (1)	0.0268 (4)	0.0286 (4)	0.0354 (5)	0.0000 (6)	0.0109 (3)	0.0002 (6)
P	−1.1831 (6)	−0.2045 (5)	−0.9579 (5)	0.026 (3)	0.034 (4)	0.051 (4)	0.012 (4)	0.011 (3)	0.004 (3)
N	−1.036 (2)	−0.207 (2)	−0.957 (2)	0.04 (1)	0.05 (1)	0.09 (2)	0.03 (2)	0.05 (1)	0.03 (1)

Isotropically Refined Atoms

atom	*x*	*y*	*z*	*U*, Å²
C1	−0.812 (2)	−0.057 (1)	−0.982 (1)	0.054 (8)
C2	−0.935 (2)	−0.084 (1)	−1.052 (1)	0.058 (8)
C3	−0.904 (2)	−0.140 (1)	−1.106 (1)	0.049 (7)
C4	−0.762 (2)	−0.147 (1)	−1.070 (1)	0.07 (1)
C5	−0.705 (2)	−0.096 (1)	−0.993 (1)	0.060 (9)
C11	−0.928 (2)	−0.364 (2)	−0.995 (2)	0.067 (9)
C12	−0.891 (2)	−0.333 (2)	−1.063 (2)	0.058 (8)
C13	−0.749 (2)	−0.326 (2)	−1.024 (2)	0.052 (8)
C14	−0.699 (2)	−0.352 (2)	−0.931 (2)	0.07 (1)
C15	−0.810 (2)	−0.376 (2)	−0.914 (2)	0.07 (1)
C21	−0.813 (2)	−0.197 (2)	−0.760 (2)	0.09 (1)
C22	−0.767 (2)	−0.124 (2)	−0.779 (2)	0.08 (1)
C23	−0.643 (2)	−0.138 (2)	−0.785 (2)	0.09 (1)
C24	−0.613 (2)	−0.220 (2)	−0.770 (2)	0.08 (1)
C25	−0.718 (2)	−0.256 (2)	−0.754 (2)	0.08 (1)
C31	−1.252 (2)	−0.3032 (9)	−0.965 (1)	0.039 (6)
C32	−1.374 (2)	−0.3265 (9)	−1.034 (1)	0.07 (1)
C33	−1.414 (2)	−0.4050 (9)	−1.040 (1)	0.07 (1)
C34	−1.331 (2)	−0.4601 (9)	−0.978 (1)	0.09 (1)
C35	−1.208 (2)	−0.4367 (9)	−0.909 (1)	0.066 (9)
C36	−1.169 (2)	−0.3582 (9)	−0.902 (1)	0.068 (9)
C41	−1.198 (2)	−0.156 (1)	−0.863 (1)	0.044 (7)
C42	−1.144 (2)	−0.081 (1)	−0.840 (1)	0.052 (8)
C43	−1.152 (2)	−0.041 (1)	−0.766 (1)	0.064 (9)
C44	−1.214 (2)	−0.076 (1)	−0.715 (1)	0.057 (8)
C45	−1.267 (2)	−0.152 (1)	−0.738 (1)	0.060 (8)
C46	−1.259 (2)	−0.191 (1)	−0.812 (1)	0.058 (8)
C51	−1.301 (2)	−0.155 (1)	−1.058 (1)	0.041 (6)
C52	−1.411 (2)	−0.115 (1)	−1.057 (1)	0.056 (8)
C53	−1.494 (2)	−0.071 (1)	−1.133 (1)	0.059 (8)
C54	−1.467 (2)	−0.067 (1)	−1.210 (1)	0.051 (8)
C55	−1.356 (2)	−0.107 (1)	−1.211 (1)	0.062 (9)
C56	−1.274 (2)	−0.151 (1)	−1.135 (1)	0.041 (6)

Table V. Bond Distances (Å) for Cp_3UNPPh_3

U–N	2.07 (2)	U–C14	2.81 (2)
P–N	1.61 (2)	U–C15	2.81 (3)
U–C1	2.78 (2)	U–C21	2.76 (3)
U–C2	2.76 (2)	U–C22	2.76 (3)
U–C3	2.78 (2)	U–C23	2.78 (3)
U–C4	2.81 (2)	U–C24	2.79 (3)
U–C5	2.81 (2)	U–C25	2.78 (3)
U–C11	2.79 (2)	P–C31	1.82 (2)
U–C12	2.77 (2)	P–C41	1.81 (2)
U–C13	2.78 (2)	P–C51	1.79 (1)

Table VI. Bond Angles (deg) for Cp_3UNPPh_3

P–N–U	172 (1)	C32–C31–P	123.0 (6)
C31–P–N	111 (1)	C36–C31–P	116.6 (6)
C41–P–N	117 (1)	C42–C41–P	117.7 (6)
C51–P–N	111 (1)	C46–C41–P	122.3 (6)
C41–P–C31	106.9 (8)	C52–C51–P	121.2 (6)
C51–P–C31	104.7 (8)	C56–C51–P	118.6 (6)
C51–P–C41	104.9 (8)		

Cp_3UNPh, $Cp_3UNCHCHPH_3$ (a model for $Cp_3UNC(Me)CHPMePh_2$[2]), Cp_3UNH_2 (a model for Cp_3UNPh_2[35]), and $Cp_3UNH_3^+$. Although no structural data for uranium amine complexes are available, the hypothetical complex, $Cp_3UNH_3^+$, would serve as a model of neutral N-donor complexes such as $Cp^*_2UCl_2(\eta^1\text{-}N_2C_3H_4)$[37] or $Cp_3U(NCMe)_2^+$.[38]

(37) Eigenbrot, C. W.; Raymond, K. N. *Inorg. Chem.* **1982**, *21*, 2653–2660.

(38) Bombieri, G.; Benetello, F.; Klaehne, E.; Fischer, R. D. *J. Chem. Soc., Dalton Trans.* **1983**, *1115*–1121.

Table VII. Some Uranium–Carbon and Uranium–Nitrogen Bond Distances

compd	U ox. state	ligand charge	ligand lone pairs	U–N or U–C, Å
Cp_3UNPh[a]	V	2−	3	2.019 (6)
Cp_3UNPPh_3[b]	IV	1−	3	2.07 (2)
Cp_3UNPh_2[c]	IV	1−	2	2.29 (1)
$Cp_3UCHPMe_3$[d]	IV	1−	2	2.274 (8)
$Cp_3UC_4H_9$[e]	IV	1−	1	2.43 (2)

[a] Reference 3. [b] This work. [c] Cramer, R. E.; Engelhardt, U.; Higa, K. T.; Gilje, J. W. *Organometallics* **1987**, *6*, 41–45. [d] Cramer, R. E.; Bruck, M. A.; Edelmann, F.; Afzal, D.; Gilje, J. W.; Schmidbaur, H. *Chem. Ber.*, in press. [e] Perego, G.; Cesari, M.; Farina, F.; Lugli, G. *Acta Crystallogr., Sect. B: Struct. Crystallogr. Cryst. Chem.* **1976**, *Ba32*, 3034–3039.

Since we wished our calculations to reflect the electronic nature of the ligand, but not the bond distance which is a result of the electronic structure, we assumed a common U–N distance of 2.06 Å, realizing that it is artificially short for several of the complexes. Idealized geometries were used for NH_3 (tetrahedral) and NH_2 (H–N–H = 120°), and we employed the theoretically optimized U–N–C angles for Cp_3UNPh, 180°, and $Cp_3UNCHCHPH_3$, 170°. These latter values compare favorably to the angles observed for Cp_3UNPh, 167.4 (6)°,[3] and $Cp_3UNC(Me)CHPMePh_2$, 163 (1)°.[2] It should be noted the U–N overlap population in $Cp_3UNCHCHPH_3$ decreases slightly, by 0.004, as U–N–C bends from linear to 170° and the nonlinear U–N–C(CH-$CHPH_3$) unit is a consequence of steric repulsion between PH_3 and Cp's.

Table VIII. Selected Data for Structurally Characterized Phosphine Imide Complexes

compound	M–N, Å	metallic radius, Å	diff, Å	P–N, Å	M–N–P, deg
Cp_3UNPPh_3[a]	2.07 (2)	1.60	0.47	1.61 (2)	172 (1)
$[Cl_4NbNPPh_3]_2$[b]	1.78	1.342	0.44	1.64	171
$[Cl_4TaNPPh_3]_2$[c]	1.801 (8)	1.343	0.46	1.593 (9)	176.8 (7)
$(PhS)_4ReNPPh_3$[d]	1.743 (7)	1.283	0.46	1.634 (9)	163.1 (6)
$F_4W(NPPh_3)_2$[e]	1.825 (6)	1.304	0.52	1.594 (6)	157.2 (4)
$F_4W(NPMe_3)_2$[f]	1.823 (7)	1.304	0.52	1.609 (8)	139.1 (4)
$(Ph_3PO)(ON)Cl_3ReNPPh_3$[g]	1.855 (8)	1.283	0.57	1.630 (8)	138.5 (5)
$(Et_2PhP)_2Cl_3RuNPPhEt_2$[h]	1.855 (5)	1.246	0.61	1.571 (5)	175.0 (4)

[a] This work. [b] Reference 11. [c] Reference 17. [d] Reference 16. [e] Reference 13a. [f] Reference 13b. [g] Reference 18. [h] Reference 25.

Table IX. Composition of the U–N Overlap Population for Cp_3UNPH_3[a]

π bond		σ bond	
U $7p_\pi$–N p_π	0.065	U 7s–N n	0.061
U $6d_\pi$–N p_π	0.144	U $7p_\sigma$–N n	0.182
U $5f_\pi$–N p_π	0.099	U $6d_\sigma$–N n	0.151
U $6p_\pi$–N p_π	−0.004	U $5f_\sigma$–N n	0.054
		U $6p_\sigma$–N n	−0.048
sum	0.304	sum	0.399

[a] The orbital notations p_π, d_π, f_π, p_σ, and f_σ correspond to (x,y), (xz,yz), (xz^2,yz^2), z, z^2, and z^3 respectively.

A most interesting feature of these calculations is the linear relationship, Figure 5, between experimental U–N bond distances and calculated U–N overlap populations. The ability of the extended Hückel overlap populations to mirror even the small differences in bond lengths between Cp_3UNPPh_3 (O), $Cp_3UNC(Me)CHPMePh_2$ (P), and Cp_3UNPh (R) is particularly noteworthy. Furthermore, both U(IV) and U(V) complexes fall on the same line, indicating no discontinuity in the bonding parameters upon change of the number of electrons in the essentially nonbonding f shell. The close correlation of overlap populations with bond distance[39] underscores the value of covalent arguments in rationalizing structural and bonding features in actinide complexes.

Figure 6 summarizes π and σ components of the U–N overlap populations and atomic charges. For $Cp_3UNCHCHPH_3$ partial U–N overlap populations associated with both the N p_x and p_y are included in the total π component. The σ overlap populations of $Cp_3UNH_3^+$ and Cp_3UNH_2 have been determined by subtracting the pseudo-π components from total overlap population. The π component comprises over 40% of the total U–N overlap population in both Cp_3UNPh and $Cp_3UNCHCHPH_3$, but among these two compounds and Cp_3UNPPh_3 π bond strength, or multiple-bond character, is largest for Cp_3UNPh. An interesting note is that still greater U–N π interaction should occur in terminal nitride complexes such as $Cp_3U{\equiv}N^{(n-)}$. As of yet, this class of compounds is unknown. While the incremental change in σ-overlap population on going from $Cp_3UNH_3^+$ to Cp_3UNH_2 to Cp_3UNPh is somewhat less than that of the π-overlap population, it also parallels experimental U–N bond lengths. Consequently, U–N σ bonding is also a factor in determining U–N bond length.

While the negative charges on N vary, there is a small decrease in positive charge on U for the series $Cp_3UNH_3^+ > Cp_3UNH_2 > Cp_3UNPH_3 \simeq Cp_3UNCHCHPH_3$ due to increasing π donation from the N atoms. With Cp_3UNPh,

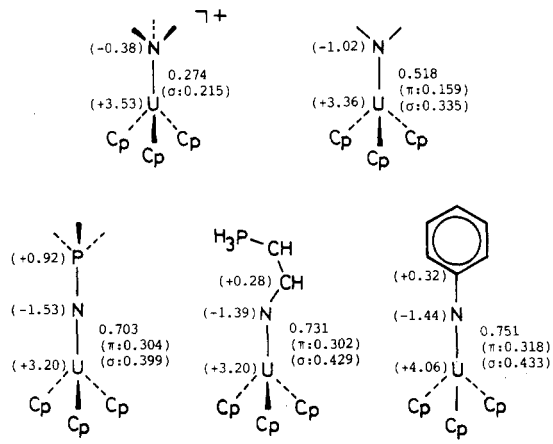

Figure 6. Summary of σ- and π-overlap populations for the U–N bonds in $Cp_3UNH_3^+$, Cp_3UNH_2, Cp_3UNPH_3, $Cp_3UNCHCHPH_3$, and Cp_3UNPh. The numbers in parentheses with signs are calculated charges on the atoms nearby.

however, a larger positive charge is localized on U, consistent with a formal (V) oxidation state, compared to U(IV) for the other complexes. Brennan and Andersen[3] suggested an f^1 electronic configuration for Cp_3UNPh, making it the first organouranium(V) complex. This view is supported by the extended Hückel calculations which indicate that only a single electron resides in the f-block molecular orbitals of Cp_3UNPh.

Comparison between the U–N Bond in Cp_3UNPH_3 and the U–O Bond in Cp_3UOPH_3. Phosphine oxides, OPR_3, are isoelectronic to phosphine imides; however the metal–oxygen bonds in phosphine oxide complexes are substantially longer than the metal–nitrogen bonds in analogous phosphine imide complexes. For example the U–O distance in $(MeC_5H_4)_3UOPPh_3$[40] is 2.389 (6) Å compared to the U–N bond distance of 2.07 (2) Å in Cp_3UNPPh_3. Also in $(Ph_3PN)ReCl_3(NO)(OPPh_3)$ the Re–O distance, 2.092 (6) Å, is longer than the Re–N separation, 1.855 (8) Å.[18] We were interested in the origin of this difference; thus, we performed extended Hückel calculations on Cp_3UOPH_3 and on a series of related complexes with model O-donor ligands: Cp_3UOH_2 (a model for $Cp_3U(THF)$[42]), $Cp_3UOCHCHPH_3$ (a model for $Cp_3UOCHCHPPh_2CH_2W(CO)_5$[43]), and Cp_3UOCH_3. In these extended Hückel calculations we fixed the U–O distance at 2.06 Å, and assumed the U–O–C angles to be

(39) The good correlation between overlap populations and bond lengths was obtained for U–C bonds as well. Tatsumi, K.; Nakamura, A. In *Applied Quantum Chemistry*; Smith, V. H., Jr., Schaefer III, H. F., Morokuma, K., Eds.; D. Reidel: Dordrecht, 1986; pp 299–311. See ref 32 also.

(40) (a) Bombieri, G.; Benetollo, F.; Bagnall, K.; Plews, M.; Brown, D. *J. Chem. Soc., Dalton Trans.* **1983**, 343–348 and references therein. (b) Casselato, U.; Fregona, D.; Tamburini, S.; Vigato, P. A.; Graziani, R. *Inorg. Chim. Acta* **1985**, *110*, 41–46. (c) Brennan, J. G.; Andersen, R. A.; Zalkin, A. *Inorg. Chem.* **1986**, *25*, 1761–1765.

(41) Cotton, F. A.; Marler, D. O.; Schwotzer, W. *Inorg. Chem.* **1984**, *23*, 4211–4215 and references therein.

(42) Wasserman, A. J.; Zozulin, A. J.; Ryan, R. R.; Moody, D. A.; Salzar, K. V. *J. Organomet. Chem.* **1983**, *254*, 305–311.

(43) Cramer, R. E.; Jeong, J. H.; Gilje, J. W. *Organometallics* **1986**, *5*, 2010–2012.

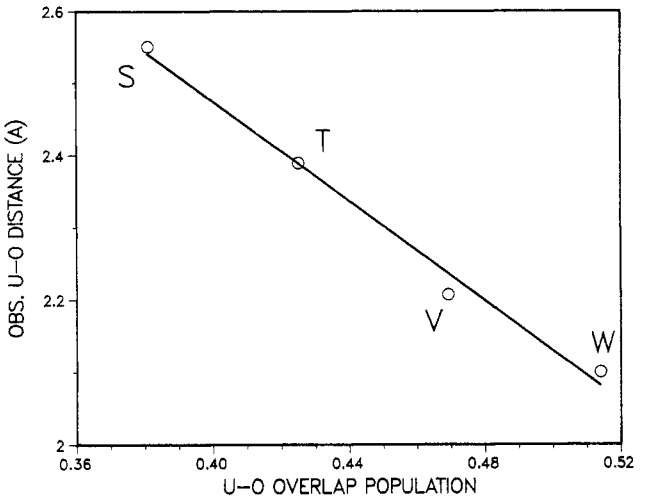

Figure 7. Correlation between the observed U–O distances and the U–O overlap populations calculated at U–O = 2.06 Å: S, $Cp_3U(THF)$–Cp_3UOH_2; T, Cp_3UOPPh_3–Cp_3UOPH_3; V, $Cp_3UOCHCHP(Ph)_2CH_2W(CO)_5$–$Cp_3UOCHCHPH_3^+$; W, $KU_2(OCMe_3)_9$–Cp_3UOCH_3.

180° in Cp_3UOPH_3 and Cp_3UOCH_3, and 156° in $Cp_3UOCHCHPH_3$.

In Figure 7 the U–O overlap populations, P(U–O), calculated for these model compounds are plotted against the observed U–O distances for the Cp_3U complexes mentioned above. Although no X-ray structure is available for Cp_3UOR, alkoxy groups are known to form short U–O bonds, as exemplified by $KU_2(OCMe_3)_9$ and $U_2(OCMe_3)_9$ where terminal U(IV)–O distances are 2.10–2.14 Å.[41] We assume the U–O bond distances in Cp_3UOR will fall in this range or, perhaps, be slightly shorter. It is evident from Figure 7 that the calculated overlap populations correlate linearly with the U–O bond lengths. Therefore variations of the observed U–O bond distances also mirror the change in covalent bond strengths derived from the extended Hückel calculations, and again two uranium oxidation states, U(III) and U(IV), fall on the same line.

Of these O-donor ligands, OCH_3^- forms the strongest U–O bond as indicated by the largest U–O overlap population, 0.514. Its π component is also large, 0.180, and comprises about 35% of the total P(U–O). However, the π component of the U–O bond in Cp_3UOCH_3 is proportionally somewhat less than in Cp_3UNPPh_3 and Cp_3UNPh, where the π components constitute 43% and 42% of the respective U–N overlap populations. Thus, for Cp_3U complexes of isoelectronic N- and O-donor ligands, our calculations indicate that U–N multiple bonding is greater than U–O multiple bonding.

As expected the P(U–O) of Cp_3UOPH_3 (T in Figure 7) is significantly smaller than that of Cp_3UOCH_3 (W in Figure 7) but is not much greater than P(U–O) in Cp_3UOH_2 (S in Figure 7). The U–O π-overlap population decreases only slightly from 0.180 to 0.165 in going from Cp_3UOCH_3 to Cp_3UOPH_3; the major decrease is in the σ population. The calculations indicate that while the σ- and π-donor orbitals of OPH_3 and NPH_3^- overlap the Cp_3U frontier orbitals in a similar way, the U–O interactions are weaker than the U–N interactions. This is partly a consequence of the more tightly bound, i.e. lower energy, OPH_3 σ and π electrons. According to the calculations the OPH_3 σ- and π-orbital levels are at −14.47 and −15.45 eV, respectively, while those for NPH_3^- are at −13.37 and −14.43 eV. Since the energy match between uranium and OPH_3 orbitals is poorer than between uranium and NPH_3^-, the U–O bond is weaker.

Table X. Parameters Used in the Extended Hückel Calculations

orbital	H_{ii}, eV	ζ_1	ζ_2	C_1[a]	C_2
U 7s	−5.50	1.914			
7p	−5.50	1.914			
6d	−5.09	2.581	1.207	0.7608	0.4126
5f	−9.01	4.943	2.106	0.7844	0.3908
6p	−30.03	4.033			
P 3s	−18.6	1.60			
3p	−14.0	1.60			
N 2s	−26.0	1.95			
2p	−13.4	1.95			
O 2s	−32.3	2.275			
2p	−14.8	2.275			
C 2s	−21.4	1.625			
2p	−11.4	1.625			
H 1s	−13.6	1.30			

[a] Exponents and coefficients used in double ζ expansion of d and f orbitals.

The P–N distance in Cp_3UNPPh_3, 1.61 (2) Å, is longer than the P–O distance, 1.492 (6) Å, in $(MeC_5H_4)_3UOPPh_3$.[40] This implies that phosphine imides are better multiple electron pair donors than phosphine oxides because resonance form L

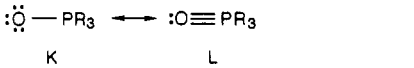

is more important in OPR_3 than J is in $[NPR_3]^-$. The calculations show a −0.97 e negative charge on the O and a +1.11 e positive charge on the P in Cp_3UOPH_3 so that the O–P bond is highly polarized. In fact, this O atom charge is nearly as negative as in Cp_3UOCH_3, −1.01 e. However, it is less than that on the nitrogen in Cp_3UNPH_3, −1.53, a result which again is consistent with the stronger, shorter bond in the phosphine imide complex.

Recently $SPPh_3$, $SePPh_3$, or $TeP(n\text{-}Bu)_3$ were found to react with $(MeC_5H_4)_3U(THF)$ to yield $(MeC_5H_4)_3U\text{–}E\text{–}U(MeC_5H_4)_3$ (E = S, Se, Te) via cleavage of the E–PPh_3 bonds.[40c] In contrast, the reaction between $OPPh_3$ and $(MeC_5H_4)_3U(THF)$ failed to give an analogous μ-O complex but instead resulted in the adduct $(MeC_5H_4)_3UOPPh_3$.[40c] Similarly, $(C_5Me_5)_2Sm(THF)_2$ reacts with $OPPh_3$ to form $(C_5Me_5)_2Sm(OPPh_3)(THF)$, while reactions with NO, N_2O, $CH_3CH_2CHCH_2O$, or C_5H_5NO yield $(C_5Me_5)_2Sm\text{–}O\text{–}Sm(C_5Me_5)_2$.[44] The failure of $OPPh_3$ to undergo O–P bond fission probably results from its strong O–P bond and relatively weak U–O bond. If this is the case, the presence of the strong U–N bond and the highly polarized N–P bond in Cp_3UNPPh_3 may imply that under proper conditions a nitride complex such as $Cp_3UN^{(n-)}$ or $(Cp_3U)_2N^{(n-)}$ might be generated by P–N cleavage in Cp_3UNPPh_3.

Appendix

Extended Hückel calculations were performed by using the quasi-relativistic uranium parameters from previous work.[45] They are listed in Table X together with the standard H, C, N, O, and P parameters. The modified Wolfsberg–Helmholz formula was used throughout. The geometrical parameters not specified in the text are as

(44) Evans, W. J.; Grate, J. W.; Bloom, I.; Hunter, W. E.; Atwood, J. L. *J. Am. Chem. Soc.* **1985**, *107*, 405–409.

(45) (a) Tatsumi, K.; Hoffmann, R. *Inorg. Chem.* **1984**, *23*, 1633–1634. (b) Tatsumi, K.; Nakamura, A.; Hofmann, P.; Stauffert, P.; Hoffmann, R. *J. Am. Chem. Soc.* **1985**, *107*, 4440–4451. (c) Hofmann, P.; Stauffert, P.; Tatsumi, K.; Nakamura, A.; Hoffmann, R. *Organometallics* **1985**, *4*, 404–406. (d) Tatsumi, K.; Nakamura, A.; Hofmann, P.; Hoffmann, R.; Moloy, K. G.; Marks, T. J. *J. Am. Chem. Soc.* **1986**, *108*, 4467–4476.

follows. Cp: C-C, 1.42 Å; C-H, 1.09 Å; Cp(centroid)-U, 2.54 Å; Cp(centroid)-U-Cp(centroid), 109.47°. NPH_3: N-P, 1.60 Å; P-H, 1.42 Å; H-P-H, 109.47°. NPh: N-C, 1.34 Å; C-C, 1.40 Å; C-H, 1.09 Å; Ph, idealized hexagon. $NCHCHPH_3$: N-C, 1.34 Å; C-C, 1.39 Å; C-P, 1.74 Å; P-H, 1.42 Å; N-C-C, 128°; C-C-P, 123°. NH_3, NH_2: N-H, 1.02 Å. OPH_3: O-P, 1.492 Å. OH_2: O-H, 1.0 Å; H-O-H, 100°. $OCHCHPH_3$: O-C, 1.33 Å; C-C, 1.40 Å; C-P, 1.71 Å; O-C-C, 118.5°. OCH_3: O-C, 1.43 Å. All the U-N and U-O distances are fixed at 2.06 Å.

Acknowledgment. The support of this work at the University of Hawaii by the National Science Foundation, Grant CHE 85-19289 (J.W.G. and R.E.C.) and by the donors of the Petroleum Research Fund, administered by the American Chemical Society (R.E.C. and J.W.G.), is gratefully acknowledged. Collaboration between Osaka University and the University of Hawaii was supported by the US/Japan Cooperative Science Program, National Science Foundation Grant INT 84-12205 (J.W.G. and R.E.C.), and a grant from the Japan Society for the Promotion of Science (K.T. and A.N.). The support of the Alexander von Humboldt Foundation through a Feodor Lynen Fellowship (F.E.) is also gratefully acknowledged.

Registry No. $LiNPPh_3$, 13916-35-3; Cp_3UNPPh_3, 112219-51-9; Cp_3UCl, 1284-81-7; $Cp_3ThNPPh_3$, 112196-30-2; Cp_3ThCl, 1284-82-8; Cp_3UNPH_3, 112196-31-3; Cp_3UNPh, 112196-32-4; $Cp_3UNCHCHPH_3$, 112196-33-5; Cp_3UNH_2, 112196-34-6; $Cp_3UNH_3^+$, 112196-35-7; Cp_3UOPH_3, 112196-36-8; Cp_3UOH_2, 112196-37-9; $Cp_3UOCHCHPH_3$, 112196-38-0; Cp_3UOCH_3, 1284-84-0.

Supplementary Material Available: Table III, positional and thermal parameters for the hydrogen atoms of Cp_3UNPPh_3 (1 page); Table IV, observed and calculated structure factors for Cp_3UNPPh_3 (14 pages). Ordering information is given on any current masthead page.

Preparation, Reactivity, Hydroformylation Catalysis, and Structural Studies of the Early Transition Metal/Late Transition Metal Heterobimetallic Complexes $Cp_2M(\mu\text{-}PR_2)_2M'H(CO)PPh_3$ (M = Zr, Hf; M' = Rh, Ir)

Lucio Gelmini and Douglas W. Stephan*

Department of Chemistry and Biochemistry, University of Windsor, Windsor, Ontario, Canada N9B 3P4

Received June 29, 1987

A series of complexes of the form $Cp_2M(\mu\text{-}PR_2)_2M'H(CO)PPh_3$ (1) have been prepared. Complexes 2-7 [M = Zr, R = Ph, M' = Rh (2); M' = Ir (3); R = Cy, M' = Rh (4); M = Hf, R = Ph, M' = Ir (5); M' = Rh (6); R = Cy (7)] have been characterized by IR, UV-vis, $^{31}P\{^1H\}$ NMR, and ^1H NMR spectroscopy. Compound 2 crystallizes in the monoclinic space group $P2_1/n$ with a = 16.398 (3) Å, b = 20.953 (6) Å, c = 13.560 (4) Å, β = 103.48 (2)°, and Z = 4. The hafnium analogue of 2 (i.e., 6) is isostructural to 2 and also crystallizes in the space group $P2_1/n$ with a = 16.372 (2) Å, b = 20.931 (4) Å, c = 13.588 (3) Å, β = 103.68 (1)°, and Z = 4. Substitution reactions involving replacement of the phosphine bound to Rh in 2 with either more basic phosphines (PEt_3, PCy_3) or CO have been studied. The substitution products $Cp_2Zr(\mu\text{-}PPh_2)_2RhH(CO)PR_3$ [R = Et (8), R = Cy (9), and $Cp_2Zr(\mu\text{-}PPh_2)_2RhH(CO)_2$ (10)] have been characterized. Compound 2 is a catalyst precursor for the catalysis of the hydroformylation of 1-hexene. Although the rate of catalysis is slower for this heterobimetallic catalyst than for related monometallic Rh species, the selectivity for terminal aldehydes is significantly greater. Aspects of the mechanism of catalysis are discussed in light of the structural and chemical data, and the role of the early metal in this chemistry is considered.

Introduction

Heterobimetallic complexes have been the subject of numerous recent studies.[1-39] In particular, interest has focused on the complexes containing early, electron-deficient and late, electron-rich metal centers. Such systems

(1) Casey, C. P.; Jordan, R. F.; Rheingold, A. L. *J. Am. Chem. Soc.* **1983**, *105*, 665 and references therein.
(2) Ho, S. C. H.; Strauss, D. A.; Armantrout, J.; Schafer, W. P.; Grubbs, R. H. *J. Am. Chem. Soc.* **1984**, *106*, 2210.
(3) Besecker, C. J.; Day, V. W.; Klemperer, W. G.; Thompson, M. R. *J. Am. Chem. Soc.* **1984**, *106*, 4125.
(4) McLain, S. J. *J. Am. Chem. Soc.* **1983**, *105*, 6355.
(5) Butts, S. B.; Strauss, S. H.; Holt, E. M.; Stimson, R. E.; Alcock, N. W.; Shriver, D. F. *J. Am. Chem. Soc.* **1980**, *102*, 5093.
(6) Bianchini, C.; Meli, A. *J. Am. Chem. Soc.* **1984**, *106*, 2698.
(7) Ritchey, J. M.; Zozulin, A. J.; Wrobleski, D. A.; Ryan, R. R.; Wasserman, H. J.; Moody, D. C.; Paine, R. T. *J. Am. Chem. Soc.* **1985**, *107*, 501.
(8) Martin, B. D.; Matchett, S. A.; Norton, J. R.; Anderson, O. P. *J. Am. Chem. Soc.* **1985**, *107*, 7952.
(9) Sartain, W. J.; Selegue, J. P. *J. Am. Chem. Soc.* **1985**, *107*, 5818.
(10) Casey, C. P.; Palermo, R. E.; Jordan, R. F.; Rheingold, A. L. *J. Am. Chem. Soc.* **1985**, *107*, 4597.
(11) Casey, C. P.; Palermo, R. E.; Rheingold, A. L. *J. Am. Chem. Soc.* **1986**, *108*, 549.
(12) Ortiz, J. V. *J. Am. Chem. Soc.* **1986**, *108*, 550.
(13) Tso, C. T.; Cutler, A. R. *J. Am. Chem. Soc.* **1986**, *108*, 6069.
(14) Casey, C. P.; Jordan, R. F.; Rheingold, A. L. *Organometallics* **1984**, *3*, 504.
(15) Barger, P. T.; Bercaw, J. E. *Organometallics* **1984**, *3*, 278.
(16) Mayer, J. M; Calabrese, J. C. *Organometallics* **1984**, *3*, 1292.
(17) Choukroun, R.; Gervais, D.; Jaud, J.; Kalck, P.; Senocq, F. *Organometallics* **1986**, *5*, 67.
(18) Ferguson, G. S.; Wolczanski, P. T. *Organometallics* **1985**, *4*, 1601.
(19) Casey, C. P.; Nief, F. *Organometallics* **1985**, *4*, 1218.
(20) Ruffing, C. J.; Rauchfuss, T. B. *Organometallics* **1985**, *4*, 524.
(21) Khasnis, D. V.; Bozec, H. L.; Dixneuf, P. H. *Organometallics* **1986**, *5*, 1772.
(22) Targos, T. S.; Rosen, R. P.; Whittle, R. R.; Geoffroy, G. L. *Inorg. Chem.* **1985**, *24*, 1375.
(23) Baker, R. T.; Tulip, T. H.; Wreford, S. S. *Inorg. Chem.* **1985**, *24*, 1379.
(24) Schumann, H.; Albrecht I.; Hahn, E. *Inorg. Chem.* **1985**, *11*, 985.
(25) Choukroun, R.; Gervais, D. *J. Organomet. Chem.* **1984**, *266*, C37.
(26) Erker, G.; Dorf, U.; Kruger, C.; Tsay, Y. H. *Organometallics* **1987**, *6*, 680.

0276-7333/88/2307-0849$01.50/0